University of Tehran

Earth Observation and Geomatics Engineering

Online ISSN: 2588-4360

Homepage: https://eoge.ut.ac.ir/

Integration of Multi-modal Remote Sensing Data and LSTM Techniques for Data Gap Prediction in Tehran

Mina Saleh[1], **Reza Shah-Hosseini**[2]✉, and **Armin Moghimi**[3]

1. School of Mapping and Spatial Information Engineering, Non-Profit University of Pouyandegan-e Danesh (Chaloos), Mazandaran, Iran E-mail: saleh.mina.sha@gmail.com
2. Corresponding author, School of Surveying and Geospatial Engineering, College of Engineering, University of Tehran, Tehran. E-mail: rshahosseini@ut.ac.ir
3. Department of Photogrammetry and Remote Sensing, Geomatics Engineering Faculty, K. N. Toosi University of Technology, Tehran 19967-15433, Iran. E-mail: moghimi@kntu.ac.ir

Article Info

Article type:
Research Article

Article history:
Received 2025-07-09
Received in revised form 2025-11-10
Accepted 2025-11-22
Available online 2026-06-02

Keywords:
Air pollution,
Long Short-Term Memory (LSTM),
gaseous pollutants and MODIS sensor.

ABSTRACT

Gaseous pollutants present growing challenges in major urban centers, posing serious threats to public health and the environment. In cities such as Tehran, where pollution levels are critically high, nitrogen dioxide (NO_2) and carbon monoxide (CO) play significant in environmental harm and health concerns. Conventional prediction models frequently depend on single-source datasets, overlooking the advantages that multi-source Remote Sensing (RS) data can offer in improving the accuracy of forecasts. To address this issue, We propose a novel approach using Long Short-Term Memory (LSTM) neural networks to estimate gaseous pollutant concentrations by incorporating multi-source RS data. This approach utilizes input from MODIS sensors (surface temperatures, aerosol optical depth, thermal emissivity) along with ground-based particulate matter data (PM_{10}, $PM_{2.5}$). Using a five-year dataset (January 2018–January 2024) from Tehran's air quality stations, we allocated 70% of the data for training and 30% for testing and validation. Our results reveal that the LSTM-based model outperformed existing methods like Gated Recurrent Unit (GRU), Random Forest (RF), One-Dimensional Convolutional Neural Network (1D-CNN) in predicting pollutant concentrations, with greater accuracy and reliability for forecasting. For CO, the R^2 values were 0.531 (GRU), 0.390 (1D-CNN), 0.498 (RF), 0.522 (Transformer), and 0.566 (LSTM); for NO_2, they were 0.953, 0.952, 0.907, 0.864 and 0.957, respectively. These results validate the superior performance of LSTM in capturing complex non-linear relationships in multi-source RS data for our case study. The improved model performance is beneficial for urban planning, pollution mitigation strategies, and public health protection.

Cite this article: Saleh. M., Shah-Hosseini, R., & Moghimi, A. (2025). Damage Detection using Gas Neural Network and Statistical Analysis using Very High-Resolution Imagery; Application to Beirut 2020 Explosion, *nouns Earth Observation and Geomatics Engineering*, Volume 9, Issue 2, Pages 1-16. http//doi.org/ 10.22059/eoge.2025.398306.1180

Publisher: University of Tehran.

DOI: http//doi.org/ 10.22059/eoge.2025.398306.1180

1. Introduction

Air pollution has become one of the most pressing environmental issues worldwide, significantly impacting public health, ecosystems, and climate (Bai, et al., 2018). According to the World Health Organization, 90% of the global population is exposed to harmful air quality, resulting in approximately 7 million premature deaths annually (WTO, 2022; Saleh, et al., 2024). Rapid urbanization, increased traffic, industrial activities, and climate change have exacerbated this challenge (Mirzaei, 2019; Mohamadzadeh, et al., 2024). Among the pollutants of concern, gaseous pollutants such as carbon monoxide (CO), nitrogen dioxide (NO_2), and sulfur dioxide (SO_2) are particularly important due to their harmful effects on human health and the environment.

CO, an odorless and harmful gas primarily from fossil fuel combustion, affects public health by causing headaches, dizziness, and even premature death (Cheng-Hong Yang et al., 2024; Muthukumar et al., 2022). SO_2, produced from industrial activities and volcanic eruptions, contributes to respiratory illnesses and cardiovascular problems (Amini, 2013; Buktieff et al., 2020; Soleimany and Grubliauskas, 2020). NO_2, resulting from burning fuels, particularly from vehicular emissions, exacerbates respiratory conditions such as asthma (Rahimi, 2017; Tela and Balogun, 2021; Phuong et al., 2020).

These data indicate that the primary sources of pollutant emissions in Tehran are the transportation industry, households, and population growth, all of which have adverse effects on public health, the environment, and the economy. Long-term exposure to these pollutants negatively affects human health and affects plant growth and development (Cheng-Heng Yang et al., 2024). Prolonged exposure to these gases can lead to respiratory diseases, cardiovascular problems, and environmental degradation, underscoring the need for effective monitoring and management strategies. To assess air quality, various measurement methods are employed. The innovation of this approach lies in its ability to effectively integrate and analyze diverse data sources, ultimately contributing to more accurate air quality predictions and better-informed environmental policies forecasting pollutant emissions and regulating industrial and energy pollution policies, along with improving public transportation and traffic planning, are essential for sustainable air quality management in Tehran. Ground-based sensors provide localized data, capturing real-time air quality variations, while Remote Sensing (RS) techniques, such as those using MODIS, provide broader spatial coverage and can monitor pollutants over large areas.

The integration of ground-based sensor data with RS data can enhances the accuracy and comprehensiveness of air quality assessments, facilitating more effective pollution management. Numerous studies have used these data to understand and forecast air pollution levels, with early research often relying on statistical methods to analyze pollutant concentrations (Rahimi, 2017; Bagheri, 2023; Tela and Balogun, 2021; Soleimani and Grobeliuskas, 2020). As the field progressed, conventional machine learning techniques gained popularity, enabling more sophisticated predictive models. Recently, deep learning methods, particularly Long Short-Term Memory (LSTM) networks, have emerged as powerful tools for time series forecasting of air quality. These methods are increasingly favored for their ability to capture complex nonlinear relationships within the data, offering improved accuracy over traditional approaches. Despite advancements in air quality monitoring and modeling, significant gaps persist in the literature. Notably, while many studies have concentrated on major cities globally, there is limited research specifically focused on gas pollutant forecasting in Tehran. Previous attempts may have encountered challenges such as inadequate data integration, limited temporal resolution, or insufficient consideration of Tehran's unique urban dynamics.

In tandem with advancements in predictive modeling, it is crucial for relevant authorities to enhance public awareness about the harmful effects of air pollutants, particularly CO and NO_2. By increasing public knowledge, citizens can make informed decisions about their health and the environment impact. Authorities should focus on promoting green energy solutions and implementing strategies to minimize traffic emissions, which are significant contributors to urban air pollution. Furthermore, fostering innovation in energy-related technologies can lead to the development of cleaner and more sustainable alternatives. By adopting a comprehensive approach that combines public education, technological advancement, and sustainable urban planning, policymakers can foster a healthier environment and mitigate the impact of air pollution in Tehran.

This study aims to address these gaps by employing a novel approach that combines multi-source RS data with ground-based measurements using advanced deep learning techniques. Multi-source RS data have been utilized to better understand the relationships between inputs and outputs, improve network performance, and address the complex interactions between pollutants and their sources. In light of these identified gaps,

this research proposes the use of LSTM model to predict the concentrations of gaseous pollutants (CO and NO_2) in Tehran. The innovation of this approach lies in its ability to

effectively

integrate and analyze diverse data sources, ultimately contributing to more accurate air quality predictions and better-informed environmental policies.

1.2. Related Studies

Numerous studies have leveraged RS and field data to predict and quantify gaseous pollutant concentrations, often employing Machine Learning (ML) models to capture complex temporal dependencies effectively. For example, (Igbal, 2011) analyzed concentrations of pollutants such as PM10, nitrogen oxides (NO_X), ozone (O_3), CO_2, and SO_2 using spatial information systems and RS data. The study explored the impact of land use on pollutant levels, revealing that all monitored pollutants, except ozone, were influenced by traffic volume, thereby highlighting a direct relationship with road density. In another study, (Nilesh and Maltare, 2023) evaluated various ML techniques to forecast air quality in Ahmedabad, India. Their analysis, using data from the Central Pollution Control Board of India, demonstrated that Support Vector Machine (SVM), LSTM, and SARIMA models exhibited superior accuracy compared to other ML approaches. (Meanwhile, Mampitiya et al., 2023) assessed the performance of eight ML models, including ANN, Bi-LSTM, Ensemble, XGBoost, CatBoost, LightGBM, LSTM, and GRU, for predicting PM10 levels in Baltimore and Kandy, Sri Lanka. Their findings indicated that ensemble models outperformed deep learning-based approaches, achieving the highest predictive accuracy. (Further, Kamali Mohammadzadeh et al., 2024) employed a spatio-temporal integration of Graph Convolutional Network (GCN) and Enhanced LSTM models to predict PM2.5 concentrations. The study concluded that integrating these models yielded greater accuracy than employing single models or traditional approaches, underscoring LSTM-based models' effectiveness. In the work of (Mirzaie, 2019), the correlation coefficient (R^2) was used to evaluate neural network models in predicting concentrations of O3, CO, NO2, and SO2. The results highlighted that neural networks significantly outperformed linear regression, capturing. complex nonlinear relationships between input data and pollutant concentrations. (Phuong et al., 2020) explored air quality in the Long Son area of Vietnam using Landsat 8 satellite images. Analyzing data from 2013, 2015, and 2017, the study identified a significant uptick in pollution from 2015 onwards, demonstrating non-compliance with the Air Quality Index (AQI). In research by (Soleimany and Grubliauskas, 2020), satellite data from Terra Aqua, and Sentinel 5P were utilized to monitor pollutant concentrations in Kaunas, Lithuania.

The study found that Sentinel 5P data provided superior accuracy in tracking SO2 and NO2 levels. While the application of LSTM models in our study might not be novel, it is grounded in substantial recent research attesting to their efficacy in accurately predicting gaseous pollutant concentrations. Thus, our usage of LSTM aligns with established methodologies and capitalizes on the proven strengths of this model in air quality forecasting using multi-source RS data.

2. Study Area

The study focuses on Tehran, the capital city of Iran, located between 51° 6' and 51° 38' east longitude and 35° 34' and 35° 51' north latitude. This metropolitan area features diverse elevations, ranging from approximately 1,800 meters in the northern districts to 1,050 meters in the south. These variations, combined with Tehran's geographical position, significantly affect its air pollution dynamics. Tehran is recognized as one of the world's most polluted cities, with rising levels of gaseous pollutants like CO and NO_2 posing substantial public health risks. These challenges are intensified by vehicular emissions, industrial activities, and topographical barriers that hinder pollutant dispersion. Effective air quality management in Tehran requires precise models to predict hourly pollutant levels. Figure 1 illustrates Tehran's geographic context, highlighting areas particularly vulnerable to air quality degradation considered in this study.

3. Dataset Description

This study utilizes a comprehensive dataset to analyze air pollution dynamics in Tehran, integrating diverse sources of RS and ground-based measurements (see Table 1). Population data from FAO/GAUL (administrative boundaries) and CIESIN/GPWv4.11 (population counts) provide demographic context, aiding in the assessment of exposure risks across urban zones. Daily Land Surface Temperature (LST) from MODIS MOD11A1, scaled by 0.02, captures thermal patterns that influence pollutant dispersion. Atmospheric characteristics are further informed by Aerosol Optical Depth (AOD) data from MODIS MCD19A2_GRANULES (scale factor: 0.001), Emis_31 and Emis_32 from the MODIS sensor, and vegetation cover is assessed via NDVI from MODIS MOD13Q1 (scale factor: 0.0001), both of which contribute to understanding pollutant absorption and movement. Ground-based monitoring stations supplied daily concentrations of key air pollutants, including NO_2, CO, SO_2, and $PM_{2.5}$, which were used as reference data for model calibration. Data were collected from 21 urban locations across Tehran— including areas such as Shahr-e Rey, Sharif University, Mahallati Highway, Doros, and several municipal districts—ensuring broad spatial coverage. To prepare the data for modeling, outliers

were removed, and a Kalman filter was applied to smooth the time series. The dataset covers daily measurements of atmospheric CO and NO_2 from January 2018 to December 2023. Digital Elevation Model (DEM) data from the SRTM (USGS/SRTMGL1_003) were also integrated toaccount for topographical influences on air flow and pollutant accumulation. This well-curated dataset forms the foundation of the predictive modeling framework developed in this study, aimed at forecasting daily concentrations of CO and NO_2 across Tehran with improved accuracy.

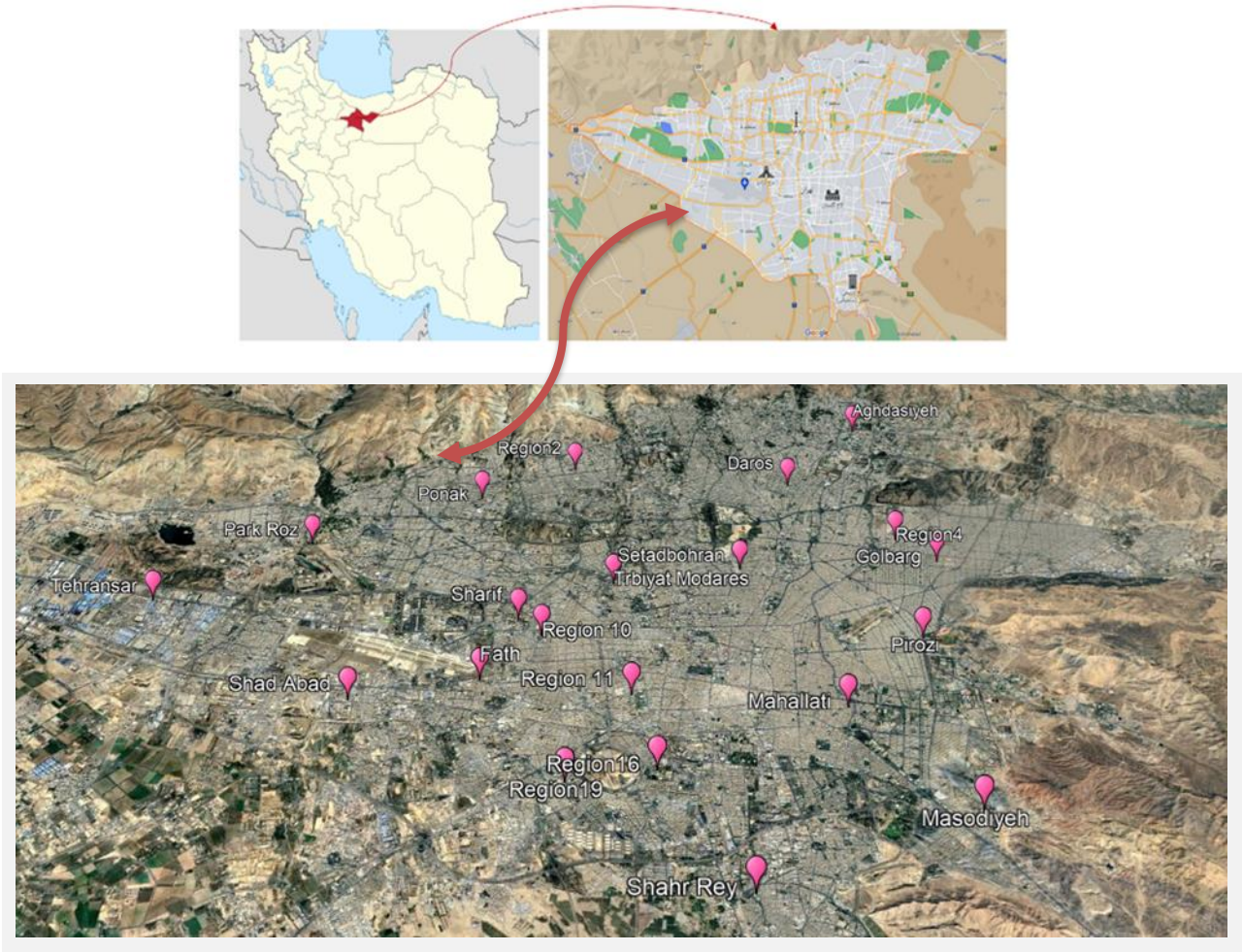

Figure 1: Geographic location of the study area—Tehran, Iran—and distribution of air pollution monitoring stations across the city.

Table 1: Characteristics of the dataset used in this Study.

Data Source	Scaling Factor	Temporal Resolution (Days)	Scaling Factor
FAO/GAUL/2015/level2	--	30	Population
MODIS/061/MOD11A1	0.02	1	LST_Day_Night_1km
MODIS/061/MCD19A2_GRANULES(Aerosol Optical Depth)	0.001	1	Optical_Depth_047
MODIS/061/MOD13Q1	0.0001	8	NDVI
MODIS/061/MOD11A1	0.002	1	Emissivity Band 31 (Emis_31)
MODIS/061/MOD11A1	0.002	1	Emissivity Band 32 (Emis_32)
CIESIN/GPWv411/GPW_Population_Count	--	--	Population
Ground-Based air quality monitoring stations	1	1	NO_2, SO_2, CO, $PM_{2.5}$, PM10, O_3, NO, NO_X
USGS/SRTMGL1_003	--	--	Elevation (DEM)

4. Methodology

In this study, we developed an ML-based model aimed at predicting the daily concentrations of NO_2 and CO in Tehran. The framework of our model is depicted in Fig. 2. To achieve this, we utilized a comprehensive dataset integrating various sources of data. This dataset combined multi-source RS variables (LST, NDVI, elevation, and AOD, Emis_31 and Emis_32) with ground-based air quality measurements such as NO_2, SO_2, CO, PM2.5, PM10, O_3, NO, and NOx. Within this dataset, the measured values of NO_2 and CO served as the target outputs for model training. Following data collection, we employed a systematic approach to categorize, preprocess, and normalize the input data. Using the powerful capabilities of GEE (Shami, et al., 2022), we ensured the dataset was accurately aligned both spatially and temporally. We addressed any incomplete or missing records using interpolation techniques and standardized all features to maintain consistency across the dataset. This prepared dataset was then divided into three subsets: 70% was allocated to training, 10% to validation, and 20% to testing, thereby ensuring a robust and unbiased evaluation of the model. The entire modeling pipeline was implemented in Google Colab using Python, leveraging its computational efficiency and ease of integration with our chosen tools. The LSTM neural network architecture, specifically designed to capture long-term temporal dependencies, was employed as our primary model. It consisted of two hidden layers, each comprising 128 neurons, optimized to improve forecasting accuracy. Model performance was rigorously evaluated using several statistical metrics, which are detailed in subsection 4.1 To benchmark the LSTM model's effectiveness, we conducted a comparative analysis against other prominent ML algorithms. These included the RF, 1D-CNN, and GRU models, each implemented within the same framework and evaluated under identical conditions to ensure a fair comparison. This comprehensive approach allowed us to critically assess the strengths and areas for improvement in our LSTM model relative to established alternatives.

Following data collection, we employed a systematic approach to categorize, preprocess, and normalize the input data. Using the powerful capabilities of Google Earth Engine (GEE) (Shami, et al., 2022), we ensured the dataset was accurately aligned both spatially and temporally. To ensure temporal consistency, Landsat 8 data (30-day resolution) was averaged to create daily values, aligning it with the daily frequency of the MODIS and ground-based measurements. The spatially aligned datasets were then integrated into a single dataset, with all variables represented at a daily temporal resolution. Any incomplete or missing records were addressed using linear interpolation, a method chosen for its ability to preserve temporal trends in the data while minimizing the introduction of bias. The percentage of missing data across all variables was less than 10%, indicating a relatively complete dataset. This prepared dataset was then divided into three subsets: 70% was allocated to training, 10% to validation, and 20% to testing, thereby ensuring a robust and unbiased evaluation of the model. The entire modeling pipeline was implemented in Google Colab using Python, leveraging its computational efficiency and ease of integration with our chosen tools. The LSTM neural network architecture, specifically designed to capture long-term temporal dependencies, was employed as our primary model. It comprised two hidden layers, each with 128 neurons, utilizing the ReLU activation function and a dropout rate of 0.2 to prevent overfitting. The model was trained using the Adam optimizer with a learning rate of 0.001, and the loss function employed was Mean Squared Error (MSE).

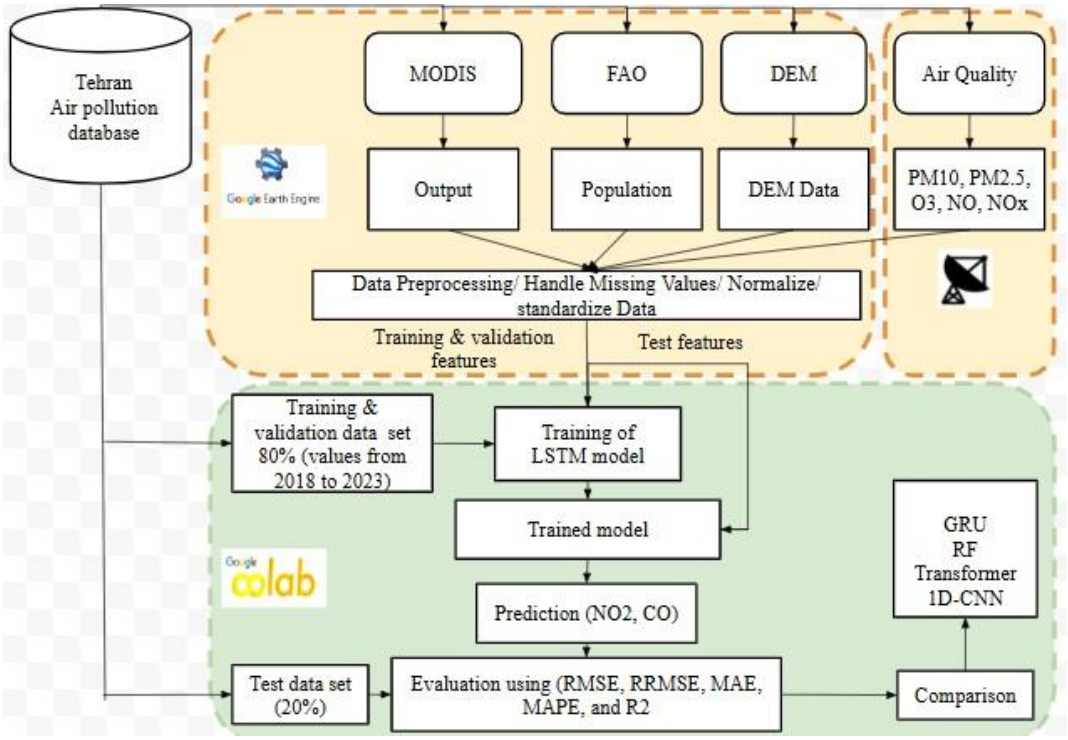

Figure (2): Proposed workflow for NO_2 and CO prediction.

4.1 LSTM

In this study, we employed the LSTM neural network as the core component of our prediction model. LSTM is a specialized type of RNN that is well-suited for capturing long-term dependencies in sequential data (Fathi, et al., 2023; Fathi, et al., 2025), making it particularly effective for time-series forecasting problems such as our task (air pollution prediction). The LSTM architecture incorporates memory cells and three key gates—input gate, forget gate, and output gate—which regulate the flow of information and allow the network to retain or discard information over long periods. This helps reduce issues like the vanishing gradient problem, which often hampers traditional RNNs.

The internal computations of a standard LSTM unit at time step are given by the following equations (Moghimi et al., 2024):

$$f_t = \delta\left(w_f \times \left[h_t - 1, x_t\right] + b_f\right) \quad (1)$$

$$i_t = \delta\left(w_i \times \left[h_t - 1, x_t\right] + b_i\right) \quad (2)$$

$$\hat{c}_t = \tanh\left(w_c \times \left[h_t - 1, x_t\right] + b_c\right) \quad (3)$$

$$c_t = f_t \times c_{t-1} + i_t \times \hat{c}_t \quad (4)$$

$$o_t = \delta\left(w_o \times \left[h_t - 1, x_t\right] + b_o\right) \quad (5)$$

$$h_t = o_t \times \tanh\left(c_t\right) \quad (6)$$

where f_t is the forget gate, σ represents sigmoid activation function, W_f and and Wo are weights, h_t-1 is the output from the previous time step, x_t is the input vector, bf, bi, and b_o are biases, Ct is the Cell state, h_t is the hidden state, and o_t is the output gate (Bouktif et al., 2020).

To train the LSTM model, we used the Mean Squared Error (MSE) as the loss function, which is standard for regression tasks like pollution level prediction. This loss function penalizes large deviations between predicted and true values, thereby guiding the model to improve its accuracy during training.

5. Experimental results

5.1. Metrics

RMSE and mean absolute percentage error (MAPE) were selected as error evaluation metrics for the model. The coefficient of determination (R^2) was used to evaluate the regression prediction results (Liu et al., 2021). The aforementioned metrics can be used to assess differences between predicted and actual values and thus can indicate the accuracy of a model. These metrics are computed as follows:

$$MAPE = \frac{1}{n}\sum_{i=1}^{N}\left|\frac{y_i - f_i}{y_i}\right| \times 100\% \quad (7)$$

$$RMSE = \sqrt{\frac{1}{n}\sum_{j=1}^{n}\left(Y_j - \hat{Y}_j\right)^2} \quad (8)$$

$$R2 = \left[\frac{\sum_{i=1}^{n}\left(\eta_{io} - \bar{\eta}_o\right)\left(\eta_{iM} - \bar{\eta}_M\right)}{\sqrt{\sum_{i=1}^{n}\left(\eta_{io} - \bar{\eta}_o\right)^2 \sum_{i=1}^{n}\left(\eta_{iM} - \bar{\eta}_M\right)^2}}\right]^2 \quad (9)$$

η_{io} is the observed air pollutants at the i_{th} time step, η_{iM} is the corresponding simulated air pollutants, n is the number of time steps, η_o is the mean of observational values, and η_M is the mean value of the simulations.

5.2 Experimental Setup

In this study, an LSTM-based model was developed separately for predicting daily concentrations of CO and NO_2, with pollutant-specific hyperparameter settings. The input time steps were 47 for CO and 48 for NO_2, using 10 input features in both cases. Models were trained using the Adam optimizer, with a batch size of 32 and dropout rate of 0.2 to mitigate overfitting. Learning rates were tuned separately: 0.00001 for CO and 0.001 for NO_2. The training process utilized MSE and RMSE as loss metrics, running for 21 epochs (CO) and 49 epochs (NO_2).

Through hyperparameter optimization, a window size of 128 and 12 LSTM units were found to yield the best results for both pollutants. The model's training and testing loss trends for both pollutants are visualized in Figure 4, where graph (a) corresponds to NO_2 and graph (b) to CO, confirming convergence and stability during training.

Table 2. LSTM hyperparameter settings for CO and NO_2 prediction.

hyperparameter	Values CO(ppm)	Values NO_2(ppm)
Input time step	47	48
Input feature dimensions	10	10
Epoch	21	49
Batch size	32	32
Learning rate	0.00001	0.001
Optimizer	Adam	Adam
Lass functions	MSE,RMSE	MSE,RMSE
Dropout	0.2	0.2

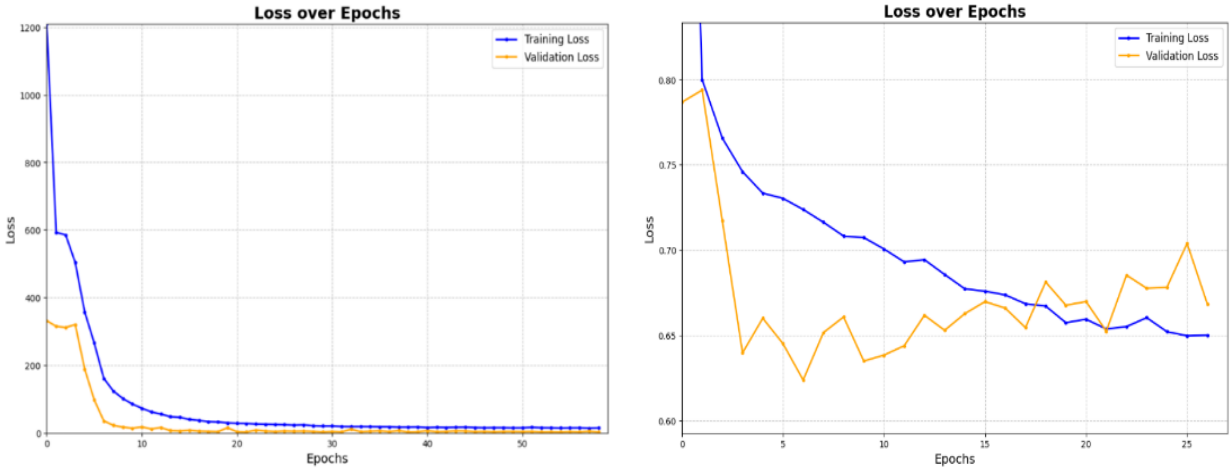

(a) (b)

Figure 3. LSTM training and testing loss curves for (a) NO_2, and (b) CO.

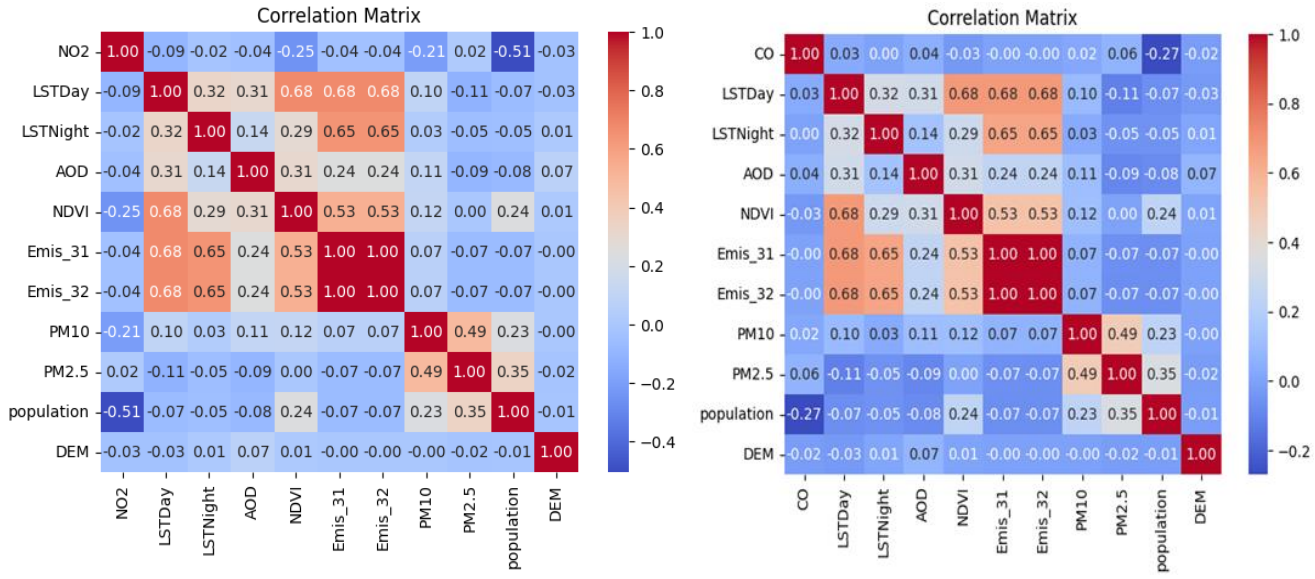

(a) (b)

Figure 4. The correlation relationships of (a) NO_2 and (b) CO with other data.

According to Figure 3, the loss curves for CO and NO_2 illustrate the LSTM model's predictive performance for pollutant concentrations in Tehran. The NO_2 loss curve initially declines rapidly, suggesting that the model effectively captures the dynamics impacting NO_2 levels, such as traffic emissions and meteorological conditions, thereby enhancing prediction accuracy. This stability, characterized by the absence of significant spikes or stagnation in the curve, reflects the model's robust understanding of complex urban influences. Conversely, the CO loss curve exhibits a steady downward trend, demonstrating the model's capability to learn and reduce discrepancies between predicted and actual CO concentrations. However, occasional fluctuations indicate external influences like sudden atmospheric changes or traffic pattern shifts, which can complicate predictions. The goal is for the loss to converge towards a minimal value, signifying the model's capacity to provide reliable CO forecasts. Additionally, a correlation analysis between RS and ground-station pollutant data inputs, illustrated in Figure 4, informed feature selection and input relevance in the modeling process. As can be seen from Figure 4, a strong positive correlation is observed between NO_2 and other pollutants such as NO and NOx, indicating that these pollutants are often influenced simultaneously by similar sources or atmospheric conditions. Additionally, remote sensing indices like AOD and LST show significant correlations with NO_2 and CO levels, likely reflecting the impact of meteorological and temperature conditions on the dispersion and accumulation of pollutants.

Regarding CO, positive correlations with particulate matter concentrations (PM2.5 and PM10) are evident, suggesting a linkage between the emission sources of CO and airborne particulate pollutants. Topographic and temperature variables also exhibit notable effects, enabling more precise modeling and improved forecasting accuracy.

5.3 Comparative Analysis of Results

Table 3 compares the predictive performance of four models—LSTM, GRU, 1D-CNN, and Random Forest—in forecasting daily concentrations of CO and NO_2. Table 4 demonstrates that the LSTM model provided the most accurate and reliable forecasts for both CO and NO_2 among the tested ML approaches, making it the preferred choice for air quality prediction in this study. From the table, it is evident that the LSTM model outperforms the other models for both pollutants. Specifically, the LSTM achieves the highest R^2 values (0.533 for CO and 0.956 for NO_2), indicating that it explains more variance in pollutant concentrations compared to GRU, 1D-CNN, Transformer and Random Forest. This suggests that LSTM is better at capturing the complex temporal dependencies inherent in the data. Moreover, the LSTM model records the lowest error metrics (MAE, RMSE, and RRMSE) for both CO and NO_2, confirming its superior accuracy. For instance, the RMSE for CO with LSTM is 0.716 ppm, which is considerably lower than GRU's 0.849 ppm, Trasformer 0.793 and Random Forest's 0.770 ppm. Similarly, for NO_2, LSTM achieves an RMSE of 3.138 ppm, outperforming GRU (3.253 ppm) and Random Forest (4.614 ppm). The lower MAPE values for LSTM (37.8% for CO and 3.05% for NO_2) further highlight its precision in predicting pollutant concentrations relative to actual values.

Figure 5 highlights how sudden spikes in NO_2 and CO concentrations are influenced by various factors. Seasonal changes, such as increased heating in colder months, can elevate CO levels, while traffic surges, particularly during peak hours, and human activities like construction and events significantly impact both NO_2 and CO levels.

Meteorological conditions, including wind, temperature, and humidity, affect pollutant concentrations through accumulation or dispersion. The introduction of new pollution sources, like factories or construction projects, as well as specific events such as fires or industrial accidents, can abruptly raise pollutant levels. Additionally, data spikes may result from technical issues like sensor malfunctions. Analyzing traffic patterns, weather conditions, and human activities, along with historical data reviews, provides insight into these fluctuations.

Table 3: Evaluation results comparing GRU, LSTM, Random Forest, and 1D-CNN models for CO and NO_2 prediction.

Metrics	LSTM (ppm)	GRU (ppm)	1D-CNN (ppm)	Transformer (ppm)	RF (ppm)	LSTM (ppm)	GRU (ppm)	1D-CNN (ppm)	Transformer (ppm)	RF (ppm)
	CO	NO2	CO	NO2	CO	CO	NO2	CO	NO2	CO
R2	**0.566**↑	**0.957**↑	0.532	0.953	0.443	**0.566**↑	**0.957**↑	0.532	0.953	0.443
MAE	**0.566**↓	**1.471**↓	0.712	1.661	0.563	**0.566**↓	**1.471**↓	0.712	1.661	0.563
MAPE	**35.203**↓	**2.969**↓	47.108	3.418	35.207	**35.203**↓	**2.969**↓	47.108	3.418	35.207
RMSE	**0.716**↓	**3.130**↓	0.849	3.251	0.717	**0.716**↓	**3.130**↓	0.849	3.251	0.717
RRMSE	**35.021**↓	**6.815**↓	50.349	6.920	37.704	**35.021**↓	**6.815**↓	50.349	6.920	37.704

As shown in Figure 5 and detailed in Table 4, prediction charts for NO_2 and CO concentrations in Tehran demonstrate the forecasting capabilities of models such as Random Forest, LSTM, GRU, Transformer and 1D-CNN. The LSTM model excels, achieving 95% accuracy for NO_2 and 53% for CO, effectively capturing complex temporal dynamics and navigating variabilities, particularly in CO, due to traffic and environmental factors. In contrast, the Random Forest and 1D-CNN models show greater discrepancies from observed values, indicating limitations under the given conditions.

Comparative analysis of results shows that the LSTM model consistently aligns closely with observed values for both pollutants, highlighting its ability to learn from historical data and adapt to dynamic urban environments. This robustness in capturing complex patterns sets LSTM apart from other models evaluated. In summary, the assessment underscores the LSTM model's superiority in forecasting NO_2 and CO concentrations in Tehran, reinforcing its potential as a critical tool for air quality management. These findings offer valuable insights for policymakers and urban planners aiming to improve air quality and public health outcomes.

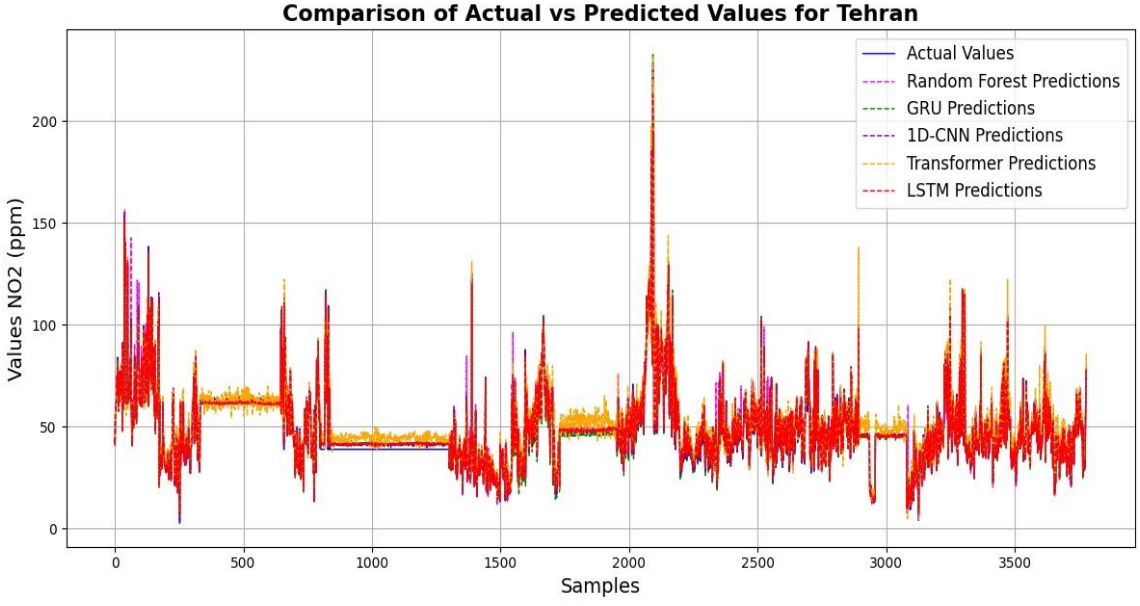

(a)

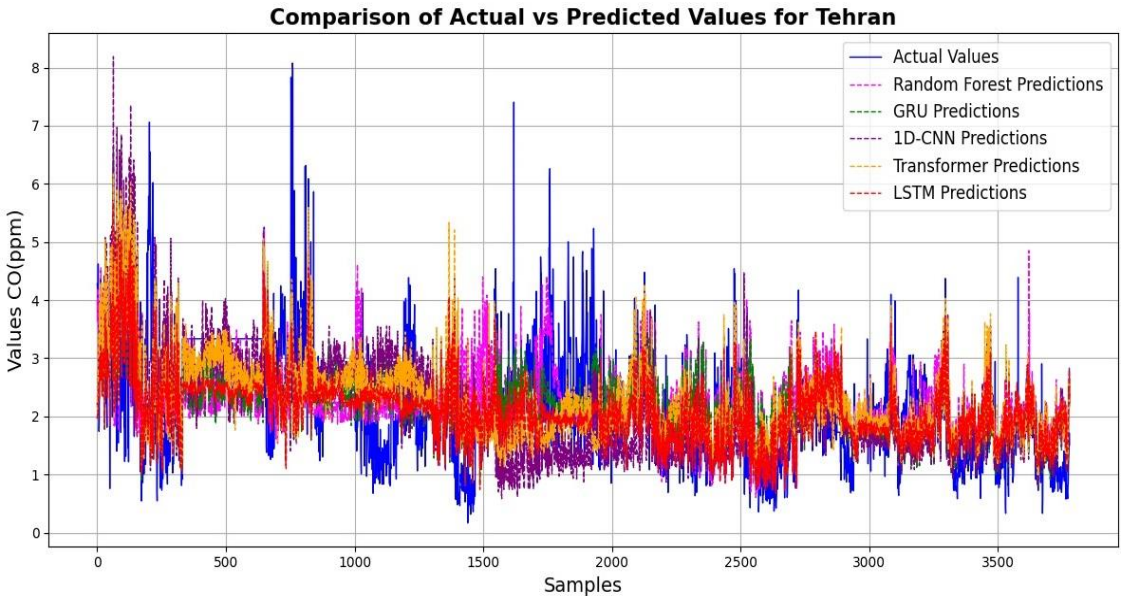

(b)

Figure. 5. Comparative forecasting of (a) NO2; (b) CO variability in 21 regions of Tehran using five predictive models.

In Figure 6, we present a scatter plot showcasing the forecasting results of NO_2 concentrations in Tehran over a 72-month period, from January 1, 2018, to December 31, 2023. This chart compares the performance of five predictive models: LSTM, 1D-CNN, GRU, Transformer and RF allowing for a comprehensive assessment of their accuracy relative to the actual NO_2 concentrations. Among the models examined, the LSTM model demonstrates the closest correspondence to the actual NO_2 values, as evidenced by the scatter points clustering tightly around the 1:1 line. This indicates a strong predictive performance where the LSTM effectively captures the temporal patterns and fluctuations in NO_2 levels. The architecture of the LSTM is particularly suited for time-series forecasting, allowing it to retain long-term dependencies and mitigate issues related to vanishing gradients. In contrast, the Random Forest model exhibits the greatest discrepancies from the actual NO_2 concentrations, with its scatter points widely dispersed from the expected values. This suggests that while Random Forest can handle varied data types, it lacks the temporal awareness necessary for accurately forecasting pollutants with dynamic seasonal patterns. The 1D-CNN model performs reasonably well, yet it shows more variability in its predictions compared to LSTM. Its ability to extract features is evident, but the model struggles with capturing the sequential dependencies crucial for accurate time-series forecasting, as indicated by the noticeable divergence of its scatter points from the actual data. Similarly, the GRU model displays moderate performance, with forecasts generally trending in the right direction, yet falling short of the precision exhibited by the LSTM. The scatter points for GRU have a broader spread compared to LSTM, indicating that while it is efficient for time-series predictions, it does not achieve the same level of consistency.

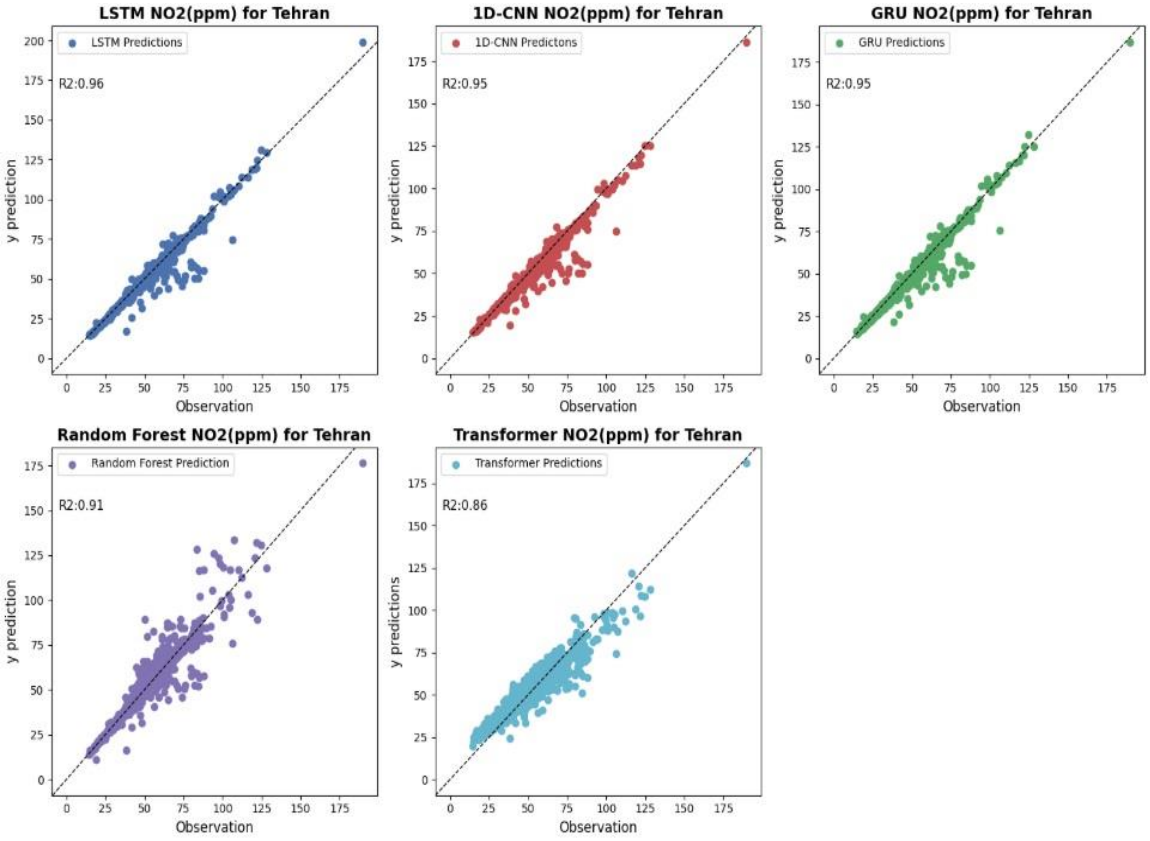

Figure 6 presents a scatter plot that showcases the forecast accuracy of NO2 concentration predictions for Tehran over a 72-month span, from January 1, 2018, to December 31, 2023. This analysis covers four predictive models: LSTM, 1D-CNN, GRU, and Random Forest (RF), Transformer.

In Figure 7, we present a scatter plot showcasing the forecasting results of CO concentrations in Tehran over a 72-month period, from January 1, 2018, to December 31, 2023. This chart compares the performance of five predictive models: LSTM, 1D-CNN, GRU, Transformer and RF allowing for a comprehensive assessment of their accuracy relative to the actual CO concentrations. Among these models, LSTM demonstrated superior forecasting performance, with scatter points that closely align with actual CO concentration measurements, underscoring its exceptional capability in capturing the temporal dynamics and trends associated with CO emissions. The LSTM's architecture, designed to manage long-term dependencies in time-series data, allows it to effectively adapt to seasonal fluctuations in air quality, thereby enhancing its suitability for pollutant forecasting. In contrast, the Random Forest model exhibits the least effectiveness, with scatter points displaying marked deviations from actual CO values. This indicates its difficulty in capturing the temporal patterns essential for accurate air quality predictions.

Although Random Forest performs well in a variety of machine learning applications, its limitations in processing time-series data, particularly for pollutants like CO with complex seasonal variability, are evident. The 1D-CNN model achieves a moderate level of accuracy, yet it lags behind LSTM. Its scatter points display slight divergences from actual concentrations, reflecting an ability to identify patterns but a deficiency in consistently handling sequential dependencies as proficiently as LSTM.

This leads to higher variance and diminished reliability for this forecasting task. Similarly, the GRU model provides moderate performance, but its precision does not match that of LSTM. The scatter chart illustrates a more noticeable spread in predicted versus actual CO concentrations. Despite GRU's design for sequence handling, its less complex structure compared to LSTM appears to inhibit its forecasting accuracy.

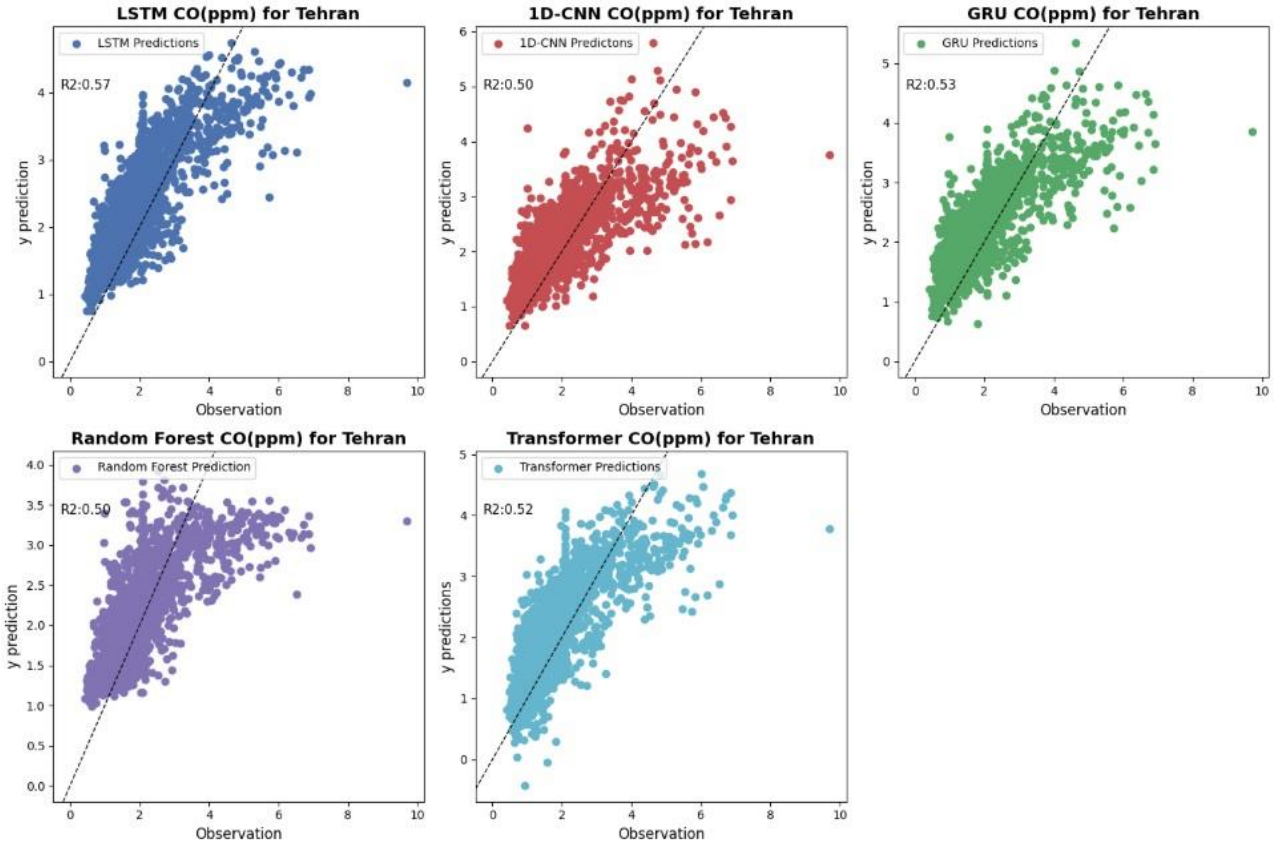

Figure 7 presents a scatter plot that showcases the forecast accuracy of CO concentration predictions for Tehran over a 72-month span, from January 1, 2018, to December 31, 2023. This analysis covers four predictive models: LSTM, 1D-CNN, GRU, and Random Forest (RF), Transformer.

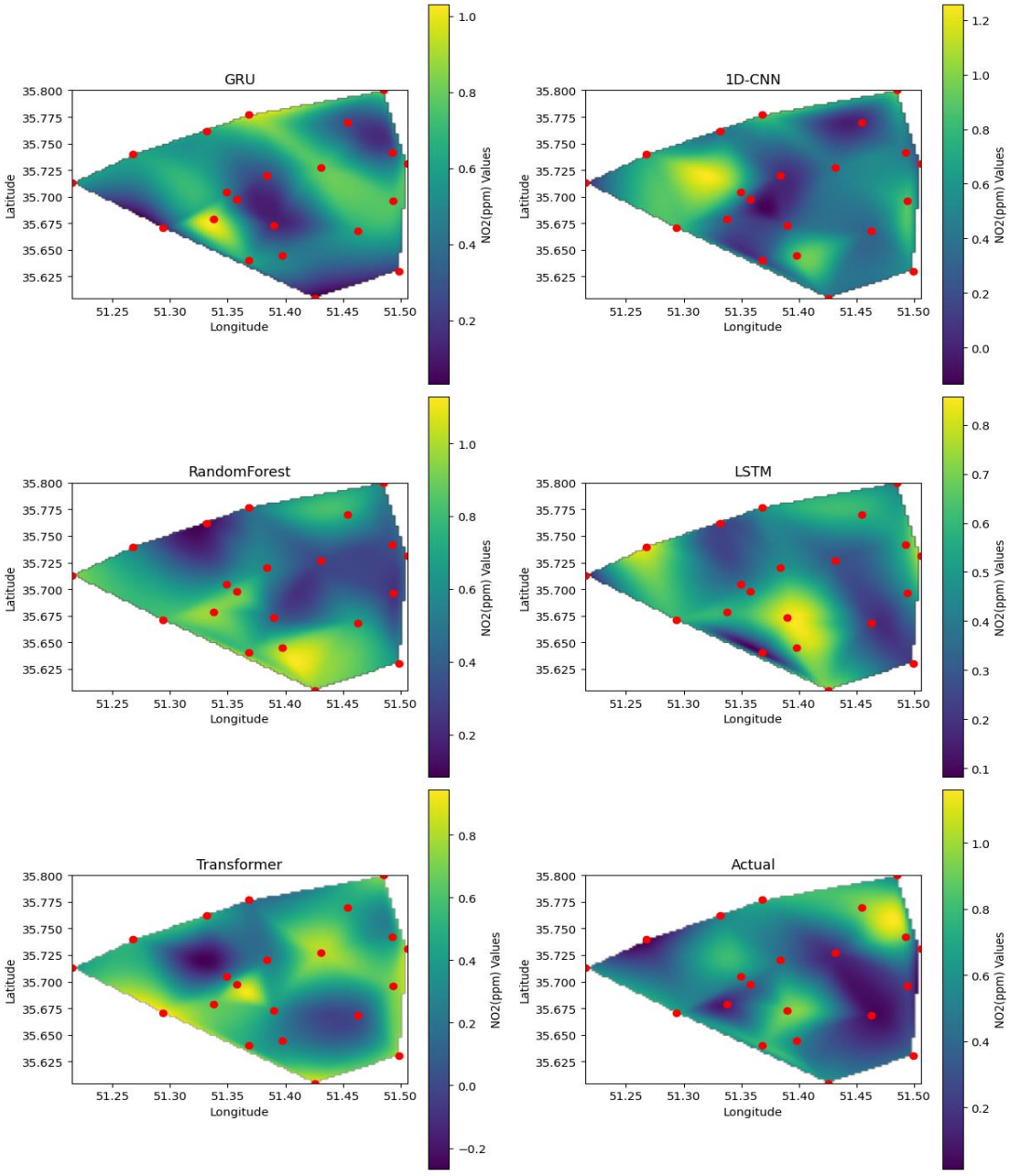

Figure 8 provides a comparative visualization of the 24-hour NO2 concentration predictions generated by LSTM, GRU, RF, 1D-CNN, and Transformer models across 21 monitoring stations in Tehran.

In Figure 8, the spatial distribution of NO_2 concentrations predicted by five different algorithms across 21 air quality monitoring stations in Tehran city is presented for the period of June 2018–2024. A color spectrum ranging from blue (low concentration) to yellow (high concentration) is used to visualize pollutant levels. These predictions are compared to the observed spatial patterns depicted in Figure 8, allowing for a comprehensive assessment of each model's performance. The LSTM model (Figure 8) demonstrates excellent accuracy, closely aligning with the observed data by effectively capturing peak concentrations in the northern and western regions while maintaining a consistent gradient of lower pollution levels towards the south and east. This consistency highlights the robustness of the LSTM model in representing both high and low concentration areas. While the LSTM and 1D-CNN models also perform well, they exhibit slight underpredictions of maximum values in the northern regions, although their overall spatial trends remain consistent with the observed data.

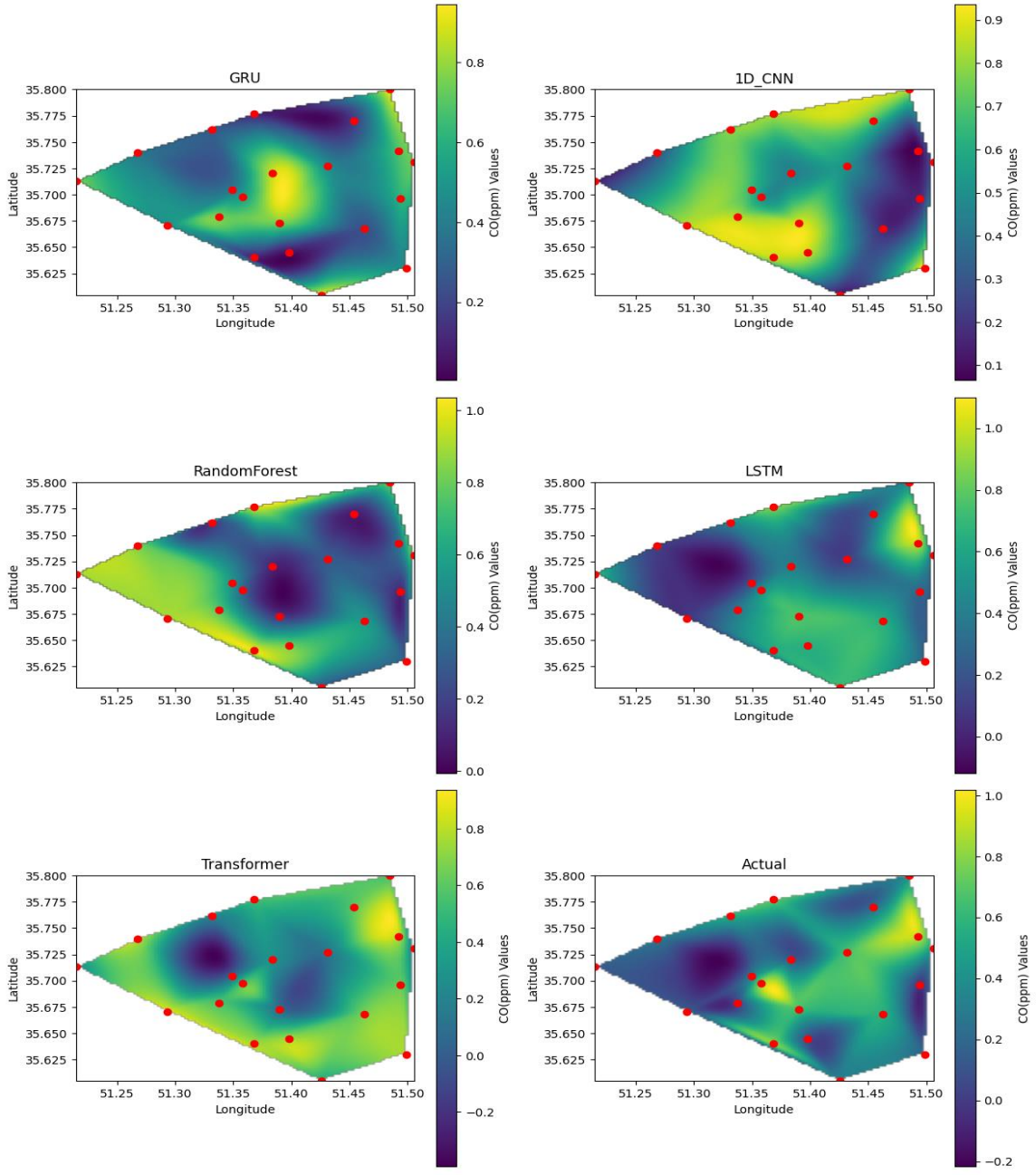

Figure 9 provides a comparative visualization of the 24-hour CO concentration predictions generated by LSTM, GRU, RF, 1D-CNN, and Transformer models across 21 monitoring stations in Tehran.

In Figure 9, the spatial distribution of CO concentrations predicted by five different algorithms at 21 air quality monitoring stations in Tehran for the period June 2018–2024 is presented. A color spectrum from blue (low concentration) to yellow (high concentration) is used to visualize pollutant levels. These predictions are compared with the observed spatial patterns in Figure 8, allowing for a comprehensive assessment of the performance of each model. The LSTM model (Figure 8) shows very good accuracy by effectively capturing peak concentrations in the northern and eastern regions while maintaining a constant slope of lower pollution levels towards the south and west, and is in close agreement with the observed data. This consistency highlights the robustness of the LSTM model in representing areas of high and low concentration. While the LSTM and GRU models also perform well, they show underpredictions of maximum values in the northern regions, although their overall spatial trends are consistent

with the observed data.

When comparing results of different models, it can be observed that LSTM produces smoother maps than Transformer, Random Forest, or 1D-CNN-based approaches. At first glance, this smoothing may appear to reduce the level of local spatial detail. However, from a methodological standpoint, this characteristic highlights one of the major strengths of LSTM: its ability to capture the dominant spatial distribution patterns of pollutants without overfitting to local fluctuations or noise. This is particularly relevant for air pollution studies, where measurement stations are sparsely distributed, and excessive local variability in the maps may not represent real environmental conditions.

6. Conclusion

This study assessed the ability of LSTM, GRU, CNN, Transformer and Random Forest models to forecast CO and NO_2 concentrations using MODIS remote sensin data and ground-based measurements from 21 stations in Tehran. The LSTM model outperformed the others, achieving the lowest Mean Absolute Percentage Error (MAPE) for CO (37.801%) and NO_2 (3.053%), demonstrating its adeptness in handling complex temporal patterns and nonlinearities. The scatter plots (see Figure 6 and 7) confirm LSTM's superior predictive accuracy and reliability over other models, especially in dynamic urban settings like Tehran. An innovative aspect of this research is the integration of remote sensing and ground data, coupled with the Adam optimization algorithm, which improved the forecasting accuracy. These results affirm LSTM's potential in air quality monitoring, informing strategies to mitigate pollution and protect public health.

Overall, although LSTM produced smoother spatial patterns compared to other models, this characteristic reflects its strength in avoiding overfitting and providing stable predictions. More importantly, its superior statistical performance (lower RMSE, MAE, and higher R^2) confirms that LSTM offers the most reliable balance between spatial plausibility and quantitative accuracy. Hence, LSTM can be considered the most effective model for pollutant interpolation and air quality assessment in this study.

Future research should consider additional metorological variables (e.g., wind speed, humidity) to enhace model performance and explore hybrid approaches combining statistical methods with machine learning for improved predictive outcomes.

References

Amini, H., Taghavi Shahri, S., Naddafi, K., Nabizadeh, R., & Yunesian, M. (2013). Correlation of air pollutants with land use and traffic measures in Tehran, Iran: A preliminary statistical analysis for land use regression modeling. *Journal of Advances in Environmental Health Research*, *1*(1), 1–8. https://doi.org/10.22102/jaehr.2013.40118

Bagheri, H. (2023). Using deep ensemble forest for high-resolution mapping of PM2.5 from MODIS MAIAC AOD in Tehran, Iran. *Environmental Monitoring and Assessment*, *195*, 451. https://doi.org/10.1007/s10661-023-10951-1

Bai, L., Wang, J., Ma, X., & Lu, H. (2018). Air pollution forecasts: An overview. *International Journal of Environmental Research and Public Health*, *15*(4), 780. https://doi.org/10.3390/ijerph15040780

Bouktif, S., Fiaz, A., Ouni, A., & Serhani, M. A. (2020). Multi-sequence LSTM-RNN deep learning and metaheuristics for electric load forecasting. *Energies*, *13*(2), 391. https://doi.org/10.3390/en13020391

Fathi, M., Shah-Hosseini, R., & Moghimi, A. (2023). 3D-ResNet-BiLSTM model: A deep learning model for county-level soybean yield prediction with time-series Sentinel-1, Sentinel-2 imagery, and Daymet data. *Remote Sensing*, *15*(23), 5551. https://doi.org/10.3390/rs15235551

Fathi, M., Shah-Hosseini, R., Moghimi, A., & Arefi, H. (2025). MHRA-MS-3D-ResNet-BiLSTM: A multi-head-residual attention-based multi-stream deep learning model for soybean yield prediction in the U.S. using multi-source remote sensing data. *Remote Sensing*, *17*(1), 107. https://doi.org/10.3390/rs17010107

Kamali Mohammadzadeh, A., Salah, H., Jahanmahin, R., Hussain, A. A., Masoud, S., & Huang, Y. (2024). Spatiotemporal integration of GCN and E-LSTM networks for PM2.5 forecasting. *Machine Learning with Applications*, *15*, 100521. https://doi.org/10.1016/j.mlwa.2023.100521

Maltare, N. N., & Vahora, S. (2023). Air quality index prediction using machine learning for Ahmedabad city. *Digital Chemical Engineering*, *7*, 100093. https://doi.org/10.1016/j.dche.2023.100093

Moghimi, A., Singha, C., Fathi, M., Pirasteh, S., Mohammadzadeh, A., Varshosaz, M., Huang, J., & Li, H. (2024). Hybridizing genetic random forest and self-attention based CNN-LSTM algorithms for landslide susceptibility mapping in Darjiling and Kurseong, India. *Quaternary Science Advances*, *100187*. https://doi.org/10.1016/j.qsa.2024.100187

Muthukumar, P., Cocom, E., Nagrecha, K., Comer, D., Burga, I., Taub, J., & Pourhomayoun, M. (2022). Predicting PM2.5 atmospheric air pollution using deep learning with meteorological data and ground-based observations and remote-sensing satellite big data. *Air Quality, Atmosphere and Health*, *15*(7), 1221–1234. https://doi.org/10.1007/s11869-021-01126-3

Rahimi, A. (2017). Short-term prediction of NO2 and NOx concentrations using multilayer perceptron neural network: A case study of Tabriz, Iran. *Ecological Processes*, *6*(4), 1–9.

Saleh, M., Shah Hosseini, R., Bahramian, Z., & Khanbani, S. (2024). A neural network-based method for real-time measurement of the concentration of golars in Tehran city using the MODIS sensor. *Geospatial Information Technology*, *4*(11), 55–81. http://jgit.kntu.ac.ir/article-1-928-fa.html

Septi Anggraini, T., Irie, H., Dimara Sakti, A., & Wikantika, K. (2024). Machine learning-based global air quality index development using remote sensing and ground-based stations. *Environmental Advances*, *15*, 100456. https://doi.org/10.1016/j.envadv.2023.100456

Shami, S., Ranjgar, B., Bian, J., Mahdi Khoshlahjeh Azar, O., Moghimi, A., Amani, M., & Naboureh, A. (2022). Trends of CO and NO2 pollutants in Iran during COVID-19 pandemic using timeseries Sentinel-5 images in Google Earth Engine. *Pollutants*, *2*(2), 156–171. https://doi.org/10.3390/pollutants2020012

Soleimany, A., & Grubliauskas, R. S. (2020). Application of satellite data and GIS services for studying air pollutants in Lithuania (case study: Kaunas city). *Air Quality, Atmosphere & Health*, *14*(3), 411–429. https://doi.org/10.1007/s11869-020-00946-z

Tella, A., Balogun, A.-L., & Faye, I. (2021). Spatiotemporal modelling of the influence of climatic variables and seasonal variation on PM10 in Malaysia using multivariate regression (MVR) and GIS. *Geomatics, Natural Hazards and Risk*, *12*(1), 443–468. https://doi.org/10.1080/19475705.2021.1879942

Thi Kim Phuong, D., Cong Nhut, M., & Duc Tri, N. (2020). Air pollution assessment using RS and GIS in Ho Chi Minh City, Vietnam: A case study of period 2015-2019 for SO2 and NO2. *IOP Conference Series: Earth and Environmental Science*, *652*, 012004. https://doi.org/10.1088/1755-1315/652/1/012004

Yang, C.-H., Chen, P.-H., Wu, C.-H., Yang, C.-S., & Chuang, L.-Y. (2024). Deep learning-based air pollution analysis on carbon monoxide in Taiwan. *Ecological Informatics*, *80*, 102477. https://doi.org/10.1016/j.ecoinf.2024.102477

Iqbal, T., "An investigation of Spatial Patterns of Urban Air Pollution and Source Recognition through GIS and Remote. Sensing in Lahore", Pakistan, 2011.

Mirzaie, M., "Modeling the concentration of air pollutants in Tehran using neural network and LUR", Shari University, Iran, 2019.